Electronic Supplementary Material (ESI) for Journal of Materials Chemistry C


# Supporting Information

Electronic Supplementary Material (ESI) for Journal of Materials Chemistry C
This journal is © The Royal Society of Chemistry 2014

# Supporting Information S1.

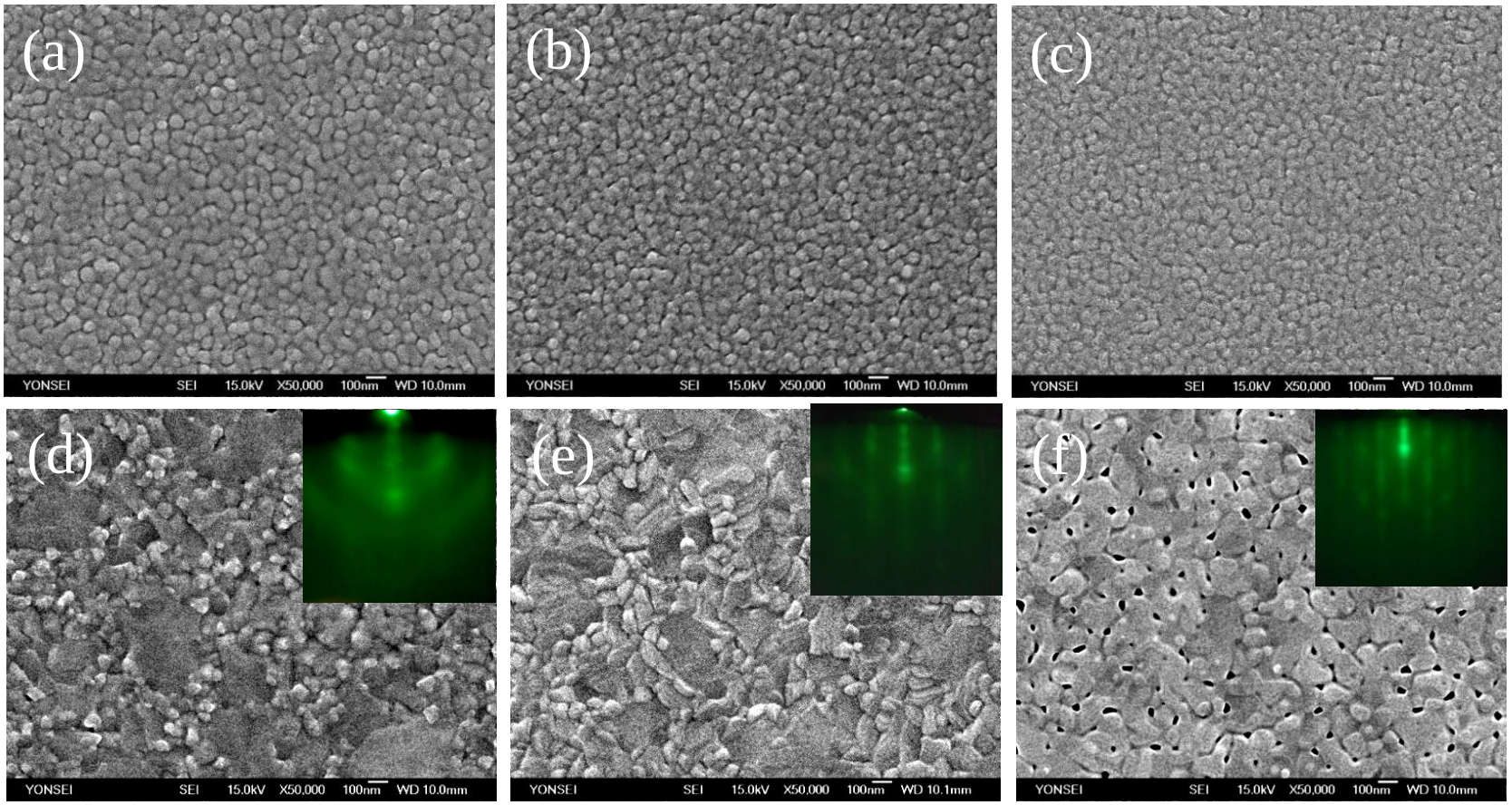


Figure S1.SEM images of the before annealing process (a)$\{Sb(3)Te(3)\}_n$, (b)$\{Sb(4)Te(6)\}_n$, (c)$\{Sb(3)Te(9)\}_n$ and after annealing process (d) $\{Sb(3)Te(3)\}_n$, (e)$\{Sb(3)Te(3)\}_n$, (f)$\{Sb(3)Te(3)\}_n$. Inset images is *in-situ* RHEED pattern.

Electronic Supplementary Material (ESI) for Journal of Materials Chemistry C
This journal is © The Royal Society of Chemistry 2013

# Supporting Information S2.

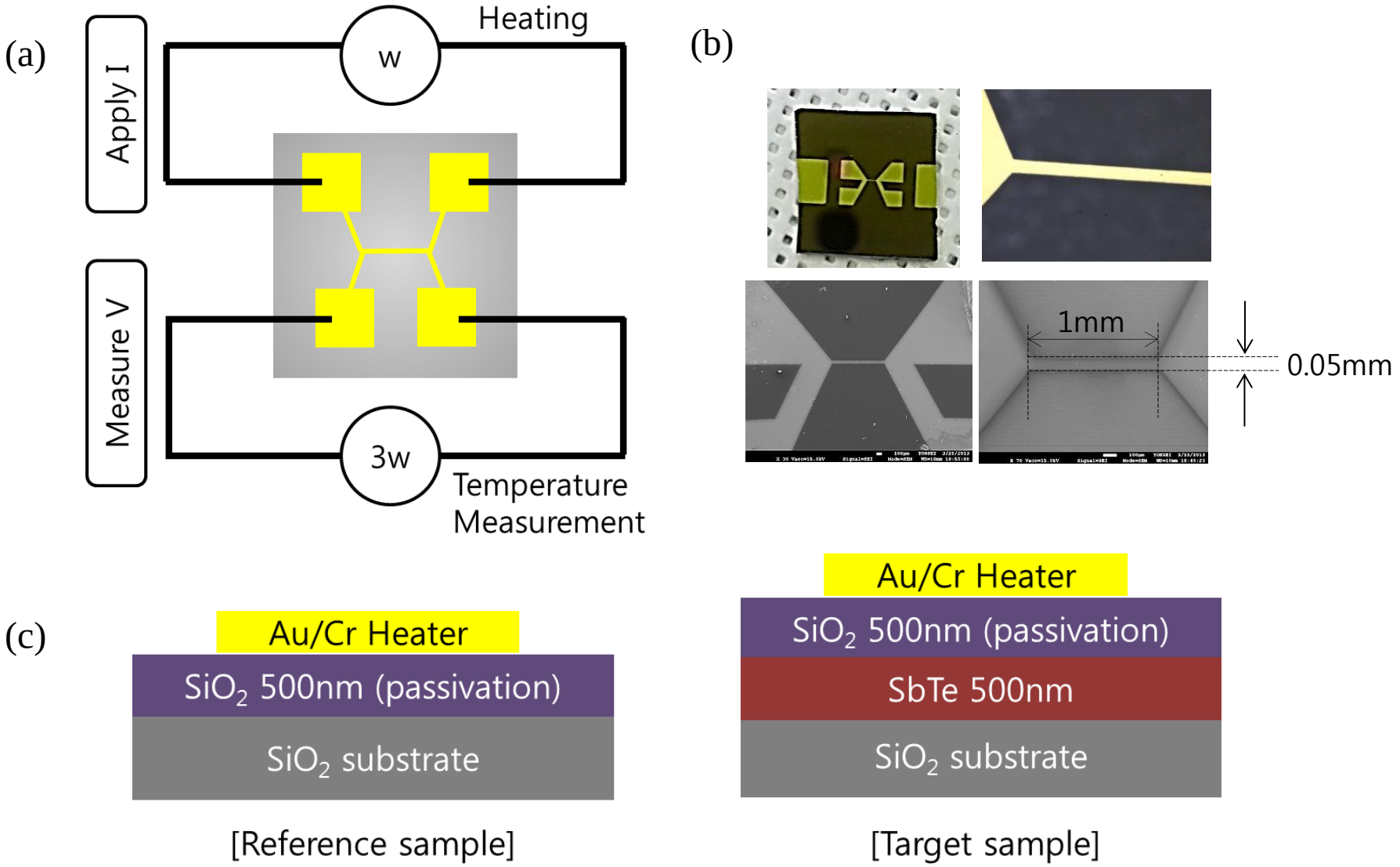


Figure S2. 3w method of thermal conductivity measurement (a)configuration of the 3w technique, (b) picture of 3w pattern sample and geometrical parameters of mask pattern (c) sample configuration for the differential 3w technique.

Electronic Supplementary Material (ESI) for Journal of Materials Chemistry C
This journal is © The Royal Society of Chemistry 2014

# Supporting Information S3.

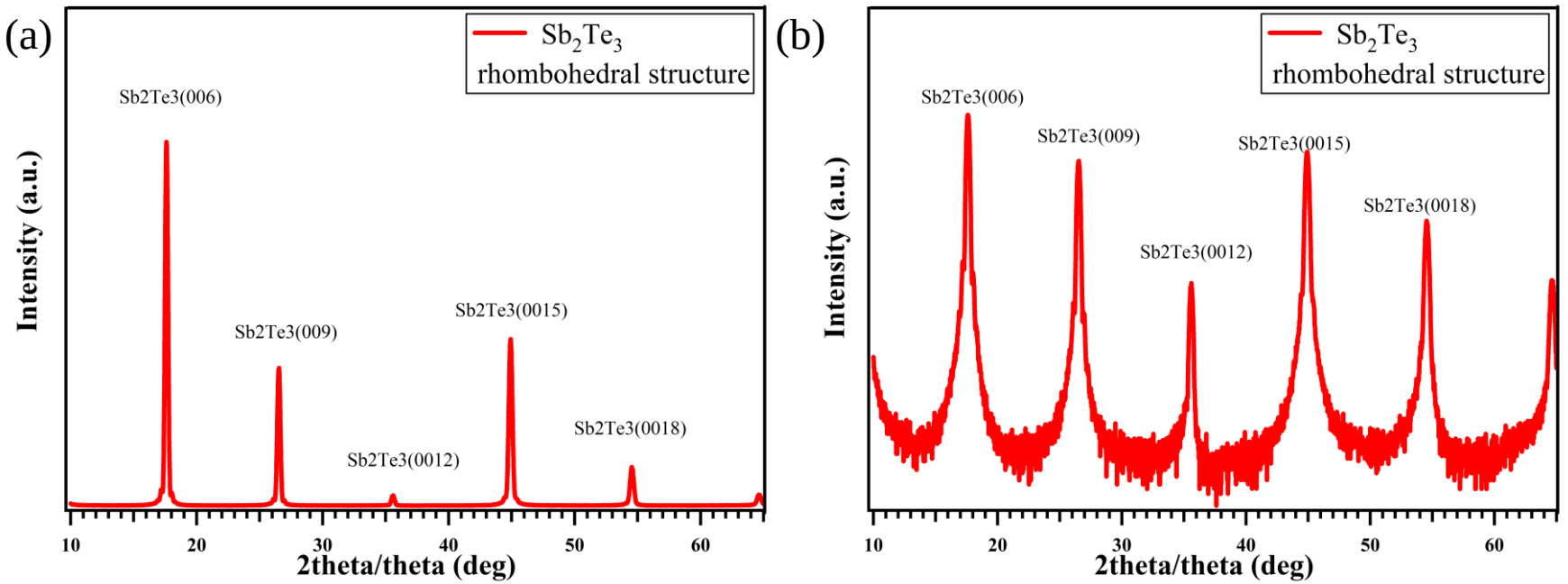


Figure S3. X-ray diffraction patterns of (a) the intensity (y-axis) scale for linear scale and (b) log scale for $\{Sb(3)Te(9)\}_n$ after annealing process. Log scale XRD patterns shows that no Te crystal phase exists.

Electronic Supplementary Material (ESI) for Journal of Materials Chemistry C
This journal is © The Royal Society of Chemistry 2014

# Supporting Information S4.

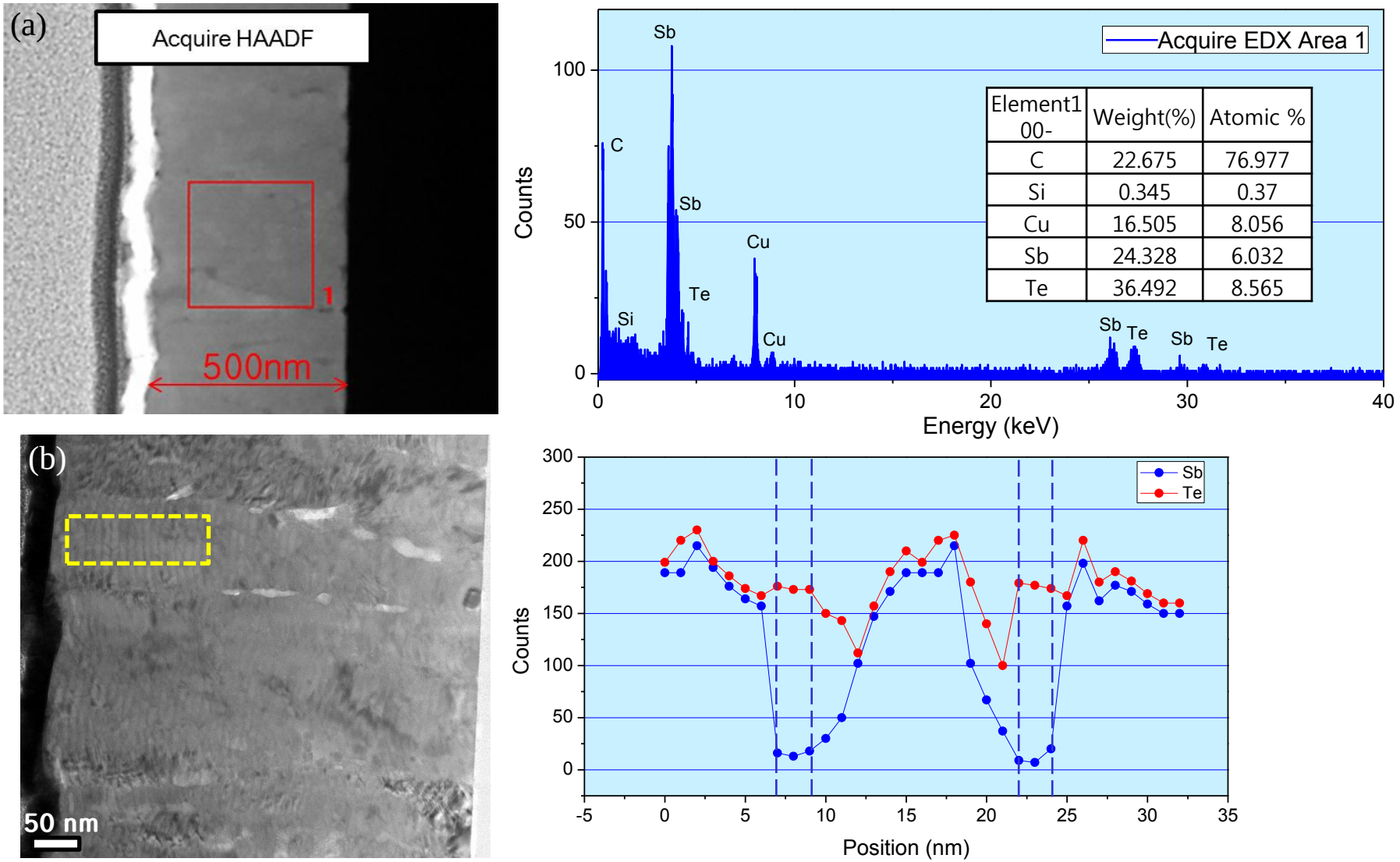


Figure S4. TEM image of $\{Sb(4)Te(6)\}_n$ after annealing process (a)HAADF STEM image and EDX spectrum obtained from sample showing the stoichiometry of $\{Sb(4)Te(6)\}_n$ sample, (b)STEM image and EDX line profile/mapping of Sb and Te elements.

Electronic Supplementary Material (ESI) for Journal of Materials Chemistry C
This journal is © The Royal Society of Chemistry 2014

# Supporting Information S5.

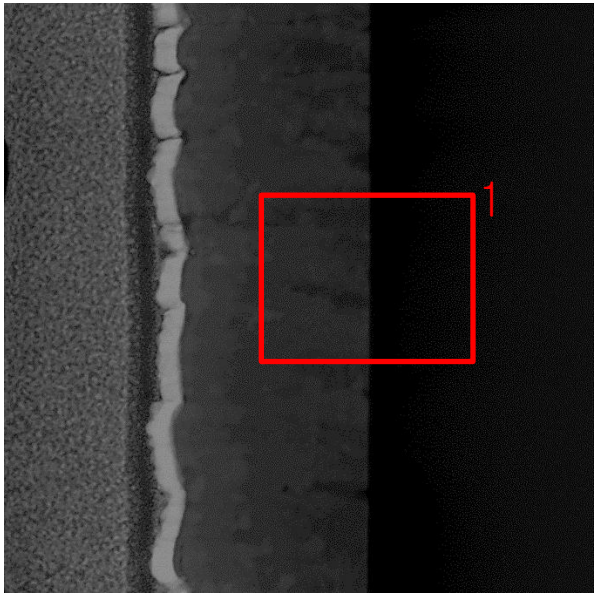


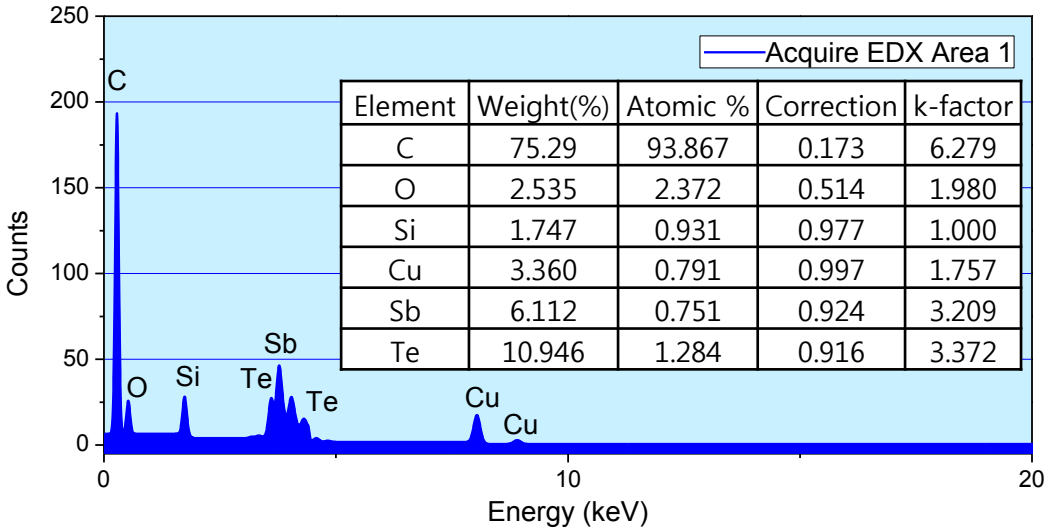


| Element | Weight(%) | Atomic % | Correction | k-factor |
|---|---|---|---|---|
| C | 75.29 | 93.867 | 0.173 | 6.279 |
| O | 2.535 | 2.372 | 0.514 | 1.980 |
| Si | 1.747 | 0.931 | 0.977 | 1.000 |
| Cu | 3.360 | 0.791 | 0.997 | 1.757 |
| Sb | 6.112 | 0.751 | 0.924 | 3.209 |
| Te | 10.946 | 1.284 | 0.916 | 3.372 |

Figure S5. TEM image of $\{Sb(4)Te(6)\}_n$ before annealing process (a)HAADF STEM image and (b) EDX spectrum obtained from sample showing the stoichiometry of $\{Sb(4)Te(6)\}_n$ sample

Electronic Supplementary Material (ESI) for Journal of Materials Chemistry C
This journal is © The Royal Society of Chemistry 2014

# Supporting Information S6.

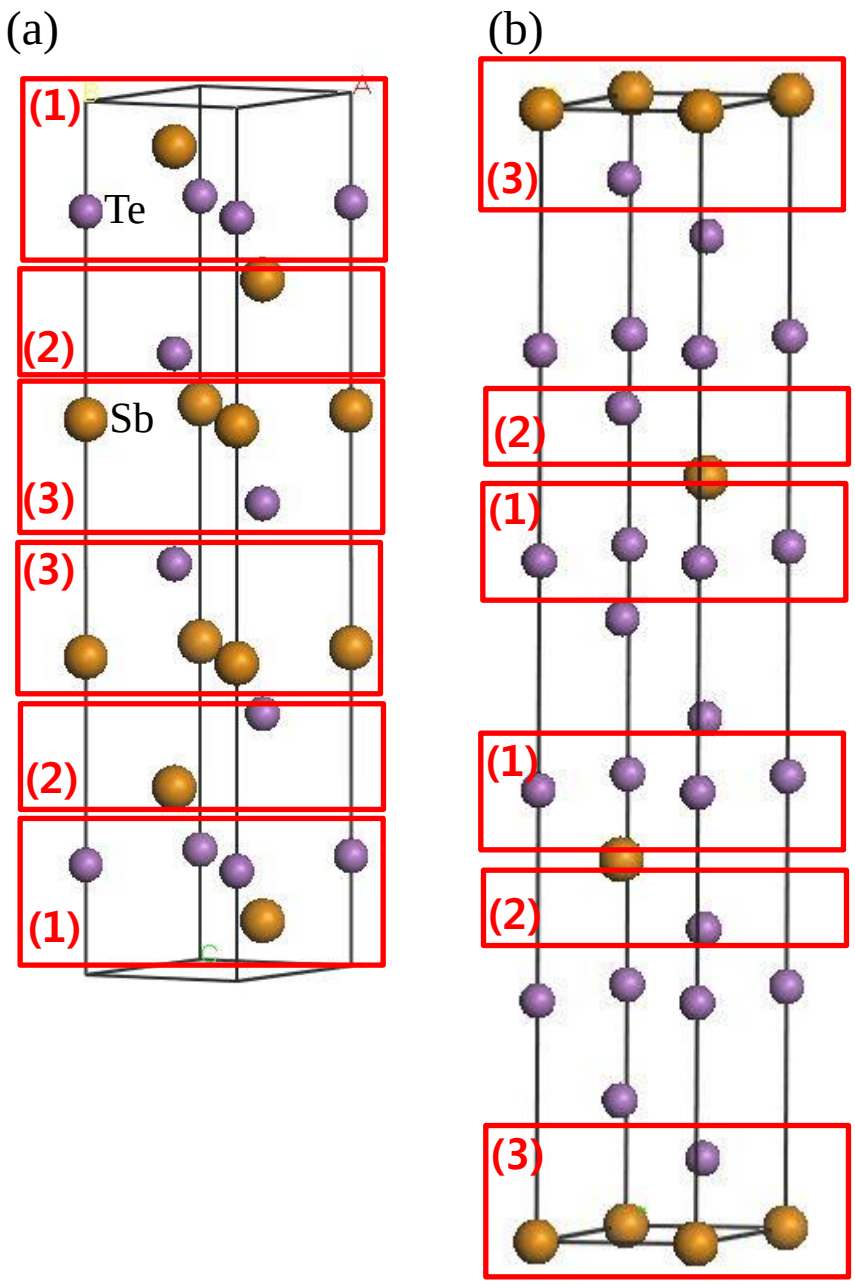


Figure S6. (a) $Sb_2Te_2$ hexagonal unit cell and (b) $Sb_2Te_3$ rhombohedral unit cell. Each of different Sb-Te Raman Vibration node denotes rectangular region with red color in (1),(2) and (3)

Electronic Supplementary Material (ESI) for Journal of Materials Chemistry C
This journal is © The Royal Society of Chemistry 2014

# Supporting Information S7.

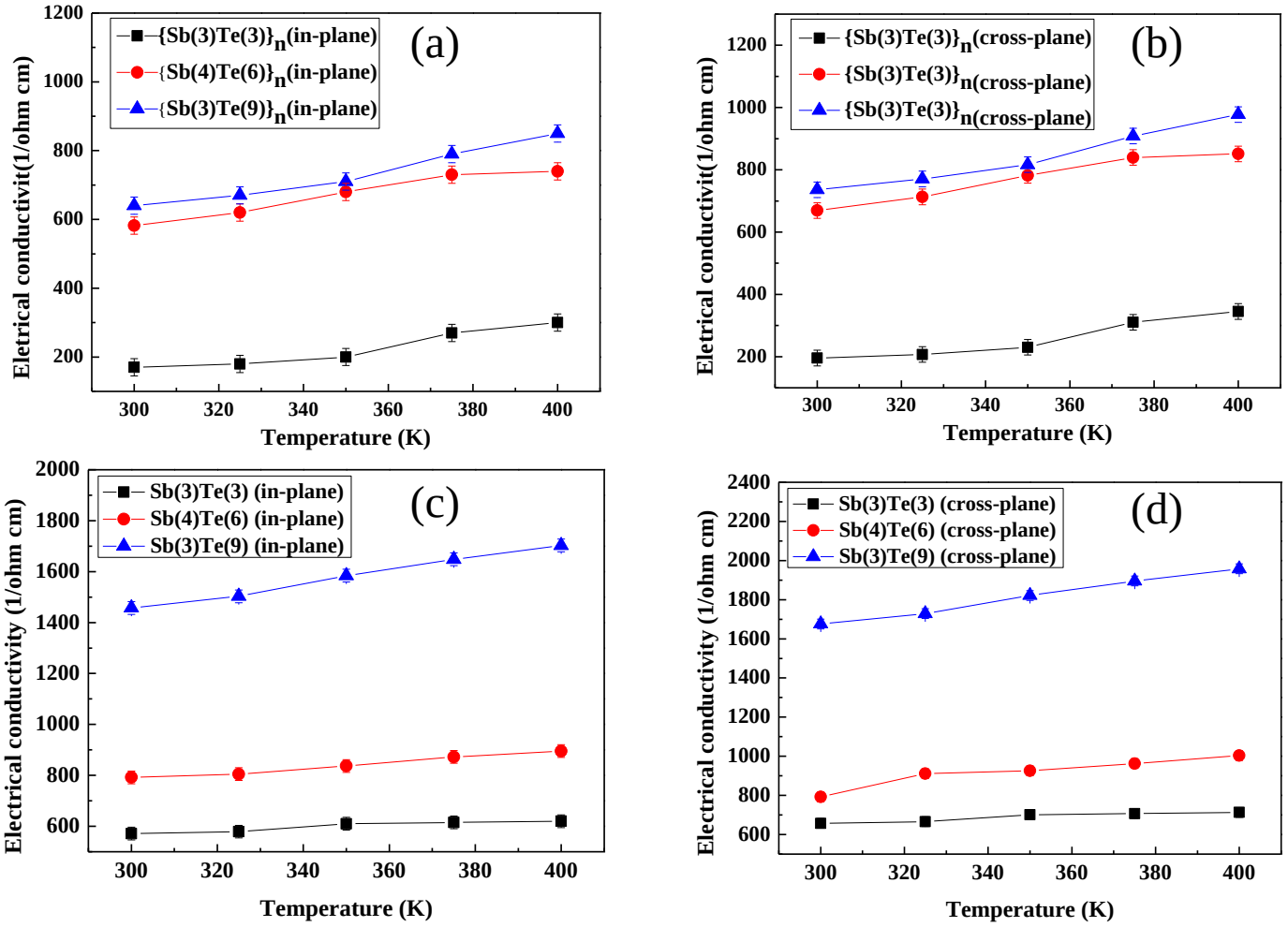


Figure S7 .Temperature dependence of electrical conductivity for (a) in-plane direction, (b) cross-plane direction of multilayered films after annealing, (c) in-plane direction and (d) cross-plane direction of co-deposited films after annealing.

Electronic Supplementary Material (ESI) for Journal of Materials Chemistry C
This journal is © The Royal Society of Chemistry 2014

# Supporting Information S8.

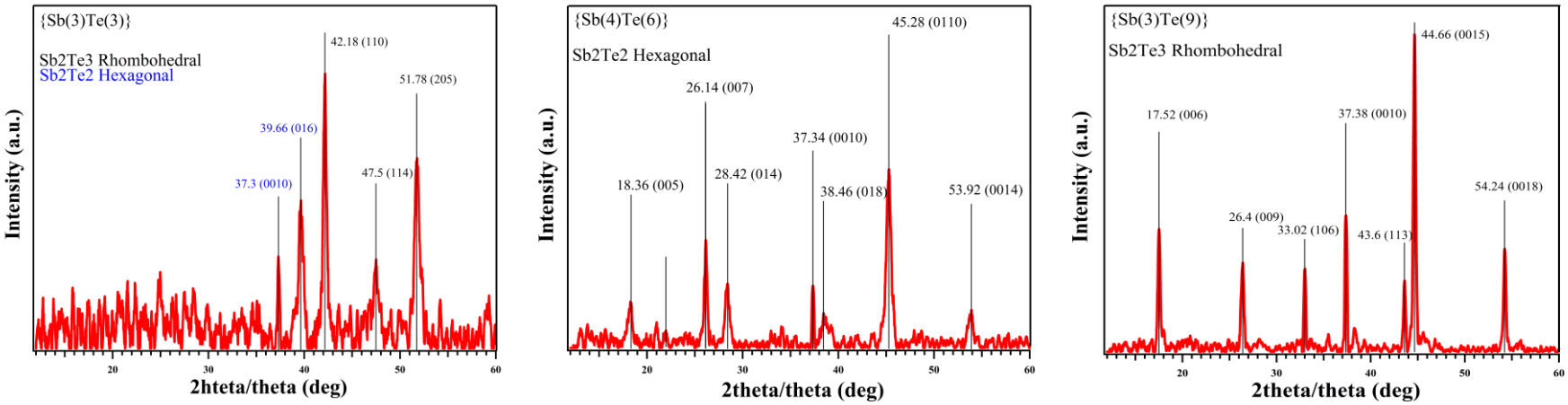


Figure S8. X-ray diffraction patterns of each co-deposited sample (a)Sb(3)Te(3), (b)Sb(4)Te(6) and (c) Sb(3)Te(9).

Electronic Supplementary Material (ESI) for Journal of Materials Chemistry C.
This journal is © The Royal Society of Chemistry 2018.

# Supporting Information Table S1.

| | | Layer | Density ($g/cm^3$) | Thickness (nm) | Roughness (nm) | Repeat |
|---|---|---|---|---|---|---|
| $\{Sb(3)Te(3)\}_n$ | as-grown | $Sb_2Te_2$ | 6.57 | 470.98 | 3.3 | 1 |
| | | $Sb_2O_3$ | 4.86 | 0.09 | 2.0 | 1 |
| | crystalline | $Sb_2Te_2$ | 5.99 | 480.39 | 4.3 | 1 |
| | | $Sb_2O_3$ | 6.33 | 1.52 | 7.7 | 1 |

| | | Layer | Density ($g/cm^3$) | Thickness (nm) | Roughness (nm) | Repeat |
|---|---|---|---|---|---|---|
| $\{Sb(4)Te(6)\}_n$ | as-grown | $Sb_2Te_2$ | 5.90 | 450.10 | 2.2 | 1 |
| | | $Sb_2O_3$ | 5.41 | 0.8 | 3.63 | 1 |
| | crystalline | $Sb_2Te_2$ | 6.65 | 10.32 | 4.32 | 40 |
| | | Te | 5.15 | 0.88 | 4.43 | |
| | | $Sb_2O_3$ | 6.08 | 6.36 | 8.358 | 1 |

| | | Layer | Density ($g/cm^3$) | Thickness (nm) | Roughness (nm) | Repeat |
|---|---|---|---|---|---|---|
| $\{Sb(3)Te(9)\}_n$ | as-grown | $Sb_2Te_2$ | 6.24 | 440.56 | 2.71 | 1 |
| | | Te | 5.15 | 0.56 | 2.69 | 1 |
| | | $Sb_2O_3$ | 6.11 | 0.16 | 5.39 | |
| | crystalline | $Sb_2Te_2$ | 6.26 | 470.68 | 5.38 | 1 |
| | | $Sb_2O_3$ | 6.88 | 0.22 | 4.82 | 1 |

Table S1. XRR fitting data for each sample in the before annealing process and after annealing process.

# Supporting Information Table S2.

| Post annealing (Crystalline) 300K | Carrier type | Carrier concentration (/cm$^3$) | Carrier Mobility (cm$^2$/Vs) | Electrical Resistivity (Ω cm) | Electrical Conductivity (1/Ω ㎝) | Seebeck Coefficient (μV/K) |
|---|---|---|---|---|---|---|
| $\{Sb(3)Te(3)\}_n$ | P | 8.4 x $10^{19}$ | 12.65 | 0.00588 | 170 | 110 |
| $\{Sb(4)Te(6)\}_n$ | P | 6.1 x $10^{20}$ | 5.96 | 0.00171 | 582 | 102 |
| $\{Sb(3)Te(9)\}_n$ | P | 3.4 x $10^{19}$ | 117.65 | 0.00156 | 640 | 127 |

Table S2. Hall measurement data and Seebeck coefficients for each sample obtained at room temperature.